



OPEN

AFP promotes cancer multidrug resistance through activating PI3K/Akt/NF-κB signaling pathway

Siren Feng^{1,4}, Chao Zhang^{1,2,4}, Yi Chen^{1,4}, Wei Li¹, Xu Dong¹, Yuli Zhou¹, Xiaowei Li¹, Fang Wang¹, Bo Lin¹, Mengsen Li^{1,3}✉ & Mingyue Zhu¹✉

Alpha-fetoprotein (AFP) has the biological function of promoting the malignant behaviors of liver cancer cells, but how it regulates drug resistance in cancer cells is still unclear. This study explores the effect of AFP on multidrug resistance (MDR) in cancers and its potential molecular mechanisms. RNA interference vector for AFP was constructed and transduced into the human liver cancer cell line Bel 7402 (high AFP expression). However, the human cervical cancer cell line HeLa (without AFP expression) was transduced with a overexpressing AFP vector. When these cancer cells were treated with doxorubicin (ADM) and 5-fluorouracil (5-FU), cell survival rate was determined by MTT, apoptosis by TUNEL, and colony formation by colony formation assay. The cancer cells were treated with the PI3K/Akt pathway inhibitor LY294002, and the expression of drug resistance-related proteins MDR1, MRP1, BCRP, Livin, cIAP1, XIAP, Akt, p-Akt, p65, and p-p65 was detected by Western blotting. Bioinformatics analysis of the correlation between AFP regulation and intracellular signaling pathways was performed. The expression and localization of p65 were observed by immunofluorescence staining. Silencing AFP could increase the sensitivity of Bel7402 cells to ADM and 5-FU, whereas AFP overexpression caused resistance to ADM and 5-FU in HeLa cells. AFP was positively correlated with the PI3K/Akt/NF-κB signaling pathway, and there was a significant difference in the correlation between p65 and drug resistance genes. AFP regulates the expression of drug resistance-related genes by activating the PI3K/Akt/NF-κB signaling pathway. AFP plays a pivotal role in MDR of cancer cells, the mechanism may be involved in activating the PI3K/Akt/NF-κB signaling pathway.

Keywords Alpha-fetoprotein, Multidrug resistance, PI3K/Akt/NF-κB, Cancer cells

Abbreviations

HCC	Hepatocellular carcinoma
CC	Cervical carcinoma
AFP	Alpha fetoprotein
MDR	Multidrug resistance
PI3K	Phosphatidylinositol 3-kinase
Akt	Protein kinase B
NF-κB	Nuclear factor kappa-B
ADM	Doxorubicin
5-FU	5-Fluorouracil
MTT	3- (4,5-Dimethylthiazol-2-yl)-2,5-diphenyl-2H-tetrazolium bromide
DMSO	Dimethyl sulfoxide
DAPI	4',6-Diamidino-2-phenylindole
FBS	Fetal bovine serum
SDS	Sodium dodecyl sulfate
PBS	Phosphate buffered saline
APS	Ammonium persulfate

¹Key Laboratory of Tropical Translational Medicine, Ministry of Education, and Hainan Provincial Key Laboratory of Carcinogenesis and Intervention, Hainan Medical University, 3 Xueyuan Road, Haikou 571199, People's Republic of China. ²Department of Pathology, Yidu Central Hospital of Weifang, Weifang 262500, Shandong, People's Republic of China. ³Department of Medical Oncology, Second Affiliated Hospital, Hainan Medical University, Haikou 570216, People's Republic of China. ⁴Siren Feng, Chao Zhang and Yi Chen contributed equally to this work. ✉email: mengsenli@163.com; mingyuezhu2002@163.com

OD Optical density

In the context of globalization, cancer has emerged as a major global health challenge, particularly for liver cancer and cervical cancer, which are characterized by high incidence rates and complex treatment regimens^{1,2}. Liver cancer, specifically hepatocellular carcinoma (HCC), poses a severe threat to public health owing to its high mortality and aggressive nature³. According to the latest global cancer statistics, liver cancer is the leading cause of cancer-related deaths⁴. Cervical cancer poses a significant health burden, particularly in developing countries⁵. Although existing treatment modalities, such as surgery, chemotherapy, and radiotherapy have improved patient survival rates to some extent, the emergence of multidrug resistance (MDR) significantly limits therapeutic efficacy, leading to cancer recurrence and poor prognosis⁶.

MDR is a phenomenon whereby cancer cells develop tolerance to one or more anticancer drugs⁷. This not only complicates cancer treatment, but also often leads to treatment failure. The mechanisms underlying MDR are complex and diverse, encompassing alterations in drug targets, increased drug efflux, decreased drug activity, among others⁷. Notably, overexpression of ATP-binding cassette (ABC) transporters is one of the key mechanisms contributing to classical MDR⁸. Alpha-fetoprotein (AFP) is an essential serum marker that plays a pivotal role in the diagnosis and treatment of HCC⁹. AFP plays a crucial role in tumor initiation and progression and is associated with various biological functions in cancer cells, including proliferation, metastasis, invasion, apoptosis inhibition, and immune evasion^{10,11}.

The present study aimed to explore the role of AFP in the development of MDR in cancer and investigate its effects on the sensitivity of cancer cells to chemotherapeutic drugs by modulating the PI3K/Akt/NF- κ B signaling pathway. By conducting experiments in AFP-positive Bel7402 HCC cell lines and AFP-negative HeLa cervical cancer cell lines, we anticipate to uncover the correlation between AFP and MDR and provide novel therapeutic strategies for reversing MDR. This research not only holds the promise of offering new insights into the treatment of liver and cervical cancers, but also has the potential to exert profound effects on the treatment of other cancer types.

Materials and methods

Cell lines and cell culture

The human HCC cell line Bel7402 (Boster Biological Technology Co., Ltd. Wuhan, China) and human cervical cancer cell line HeLa (Zhongqiao Xinzhou Biotechnology Co., Ltd., Shanghai, China) were cultured in DMEM (Dulbecco's Modified Eagle Medium, HyClone, USA) containing 10% FBS (fetal bovine serum, Gibco, USA), 50 IU/mL penicillin, and 100 μ g/mL streptomycin at 37 °C in a 5% CO₂ atmosphere. Cells were passaged every 2–3 days, and when cell confluence reached approximately 90%, 0.25% trypsin solution (Gibco, USA) was used for digestion to maintain the subclone state of the cells.

Generation, construction and transduction of AFP-expressed or interfered vectors

The full-length AFP gene with a Flag tag, short hairpin RNA (shRNA) was inserted into the lentivirus pLV[Exp]-EGFP-Puro vector¹². The AFP expression vector was named pLV-AFP-FLAG, the interfering AFP expression vector was named pLV-shAFP. Bel7402 cells were infected with pLV-shAFP, and pLV-AFP vectors were infected with HeLa cells, and stable cell clones were screened with puromycin. Cells stably expressing AFP were named HeLa-AFP, and cells that stably interfered with AFP were named Bel7402-shAFP. The transduction rate and transduction effect of the expressing or interfering vectors were verified by fluorescence microscopy and Western blotting, respectively.

Western blotting analysis

After pLV-AFP and pLV-shAFP vectors were infected with Bel7402 and HeLa, respectively, Western blotting was used to detect the expression of AFP, Akt, phosphorylated-AKT (Ser473) [p-Akt(Ser473)], MRP1/ABCC1, MDR1/ABCB1, BCRP1/ABCG2, XIAP, Livin, cIAP1, NF- κ B p65, phospho-NF- κ B p65 and β -actin proteins. The assay antibodies of AFP, MRP1/ABCC1, MDR1/ABCB1, BCRP1/ABCG2, XIAP, Livin, cIAP1, NF- κ B p65, and phospho-NF- κ B p65 were purchased from Cell Signaling Technology (Danvers, Massachusetts, USA), Akt and p-Akt antibodies were purchased from Abcam (Cambridge, USA). The detailed procedure has been previously described¹³.

MTT Assay and trypan blue exclusion dye method

After the pLV-AFP and pLV-shAFP vectors were infected into Bel7402 and HeLa cells, respectively, the cells were treated with ADM (adriamycin, Shanghai MedChemexpress Co., Ltd.) and 5-Fu (5-Fluorouracil, Shanghai MedChemexpress Co., Ltd.) at different concentration gradients. For the MTT assay¹⁴, after drug treatment for a predetermined period (e.g., 48 h or 72 h), MTT reagent was added to each well and incubated at 37 °C in a 5% CO₂ incubator for 4 h. The supernatant was then carefully aspirated, and dimethyl sulfoxide (DMSO) was added to dissolve the formazan crystals formed in viable cells. A microplate reader (BIO-RAD Laboratories, Inc., Hercules, California, USA) was used to measure the absorbance at a wavelength of 490 nm. The cell growth inhibition rate of each group was calculated using the formula: $((1 - OD \text{ value of the drug-treated group}) / OD \text{ value of the normal control group}) \times 100\%$, where the normal control group refers to cells without drug treatment and with corresponding vector infection. For trypan blue staining¹⁴, at the same time point as the MTT assay, the treated cells were gently digested with trypsin, resuspended in complete medium to form a single-cell suspension, and mixed with 0.4% trypan blue solution at a 1:1 volume ratio. After standing at room temperature for 3–5 min, the cell mixture was added to a hemocytometer. Under an inverted microscope, live cells (colorless, transparent, and with intact morphology) and dead cells (blue-stained, with irregular morphology) were counted separately. The cell viability was calculated as: $(\text{number of live cells} / (\text{number of live cells} + \text{number of dead cells})) \times 100\%$.

Colony survival assay

Colony Survival Assay was used to evaluate the long-term survival and proliferation ability of cells after drug treatment¹⁵. Cells in the logarithmic growth phase were seeded in 6-well plates at approximately 500 cells/well. After cell attachment, appropriate concentrations of ADM or 5-Fu were added to each well. After 48 h, the medium was replaced with fresh culture medium and the cells were further cultured in an incubator for 14 days. When colonies became visible to the naked eye, the medium was aspirated and the wells were thoroughly washed with PBS. Next, 4% paraformaldehyde was added to each well and the cells were fixed for approximately 30 min. After discarding the 4% paraformaldehyde, the wells were washed twice with PBS and an appropriate amount of 0.1% crystal violet was added for staining for 30 min. The 6-well plates were rinsed with tap water and air-dried before counting. Each colony contained at least 50 cells.

TUNEL detection

For apoptosis assay, 4×10^3 cells/well were seeded into 96-well plates and cultured at 37 °C with 5% CO₂ in a humidified environment. The One Step TUNEL Apoptosis Assay Kit (Beyotime) was used for detecting apoptotic cells¹⁶. Nuclei were stained with DAPI (blue). Fluorescent images were acquired by a fluorescence microscope (ECLIPSE Ts2R, Nikon). The quantification of TUNEL-positive cells was obtained by ImageJ software and calculated by GraphPad Prism version 5.0.

Bioinformatics analysis

Online resources, such as LinkedOmics, GEPPIA, DAVID, OECLOUD online enrichment tools, and Clinical Omics, were used to analyze the correlation between specific target genes, perform gene functional annotation, conduct enrichment analysis, and visualize the results.

Immunofluorescence observation

Immunofluorescence Observation was performed to visualize protein localization¹⁷. The cells were cultured at a density of 2×10^4 /mL for 24 h. After attachment, the cells were washed twice with PBS for 5 min each. Subsequently, the cells were fixed with 200 μ L 4% paraformaldehyde for 30 min, followed by two washes with PBS for 5 min each. Next, 200 μ L 0.3% TritonX-100 was added and incubated for 15 min, followed by two washes with PBS. The cells were blocked with 200 μ L of QuickBlock™ immunostaining blocking solution (Beyotime Biotechnology, Shanghai, China) for 15 min. The primary antibodies were incubated overnight at 4 °C, and the next day, the cells were washed twice with PBS. Secondary antibodies conjugated with donkey anti-rabbit IgG (Alexa Fluor® 647) were applied for 1 h at 37 °C in the dark, followed by two washes with PBS. Finally, the nuclei were stained with 100 μ L of DAPI staining solution for 20 min, and the cells were mounted using an anti-fade mounting medium. After completing the above steps, cells were observed and photographed under an inverted fluorescence microscope (Olympus Corporation, Tokyo, Japan).

Statistical analysis

Each experiment was repeated at least three times. Band intensities and colony counts were analyzed using ImageJ software. Experimental data are expressed as mean \pm standard deviation (SD). Statistical analyses were performed using SPSS 26.0 or GraphPad Prism software (version 8.0). ANOVA was used for comparisons among multiple groups, and statistical significance was set at $P < 0.05$.

Results

AFP inhibits the sensitivity of cancer cells to drug treatment

To investigate the effect of stable AFP silencing on the sensitivity of Bel7402 cells to chemotherapeutic drugs, Bel7402 cells were transduced with the LV-shAFP lentivirus (The lentiviral vector structures used to construct overexpressing AFP is shown in the supplementary materials Figure S1) or empty lentiviral vector (NC). Approximately 90% of the cells were GFP-positive at 72 h post-transduction, indicating high transduction efficiency of the lentiviral vectors (Fig. 1A-a). After puromycin selection, Western blotting analysis revealed significantly reduced AFP protein expression in Bel7402-shAFP cells compared to control Bel7402-shNC and normal Bel7402 cells ($P < 0.01$), confirming that successful establishment of a Bel7402-shAFP cell line with stable AFP silencing (Fig. 1A-b). Subsequently, MTT assays were performed to examine the sensitivity of Bel7402 cells to two chemotherapeutic drugs (ADM and 5-FU), after AFP silencing. The results showed that the growth inhibition rate of the cells gradually increased with increasing drug concentrations. Notably, at higher concentrations of ADM and 5-FU, the growth inhibition rate of Bel7402-shAFP cells was significantly higher than that of normal Bel7402 and Bel7402-shNC cells ($P < 0.01$ or $P < 0.05$) (Fig. 1A-c, d). Trypan blue staining further confirmed a significant decrease in cell viability after AFP silencing (Fig. 1A-e, f). Furthermore, colony formation assays were used to evaluate the clonogenic ability of cells after drug treatment. In the drug treatment groups containing 0.2 μ g/mL ADM and 5 μ g/mL 5-FU, the number of colonies formed by Bel7402-shAFP cells was significantly reduced compared to that in the normal Bel7402 and Bel7402-shNC cells ($P < 0.01$) (Fig. 1A-g, h). These findings suggest that interference with AFP expression in HCC cells can significantly enhance the sensitivity of Bel7402 cells to ADM and 5-FU.

To investigate the effect of AFP overexpression on the chemosensitivity of cervical cancer cells, HeLa, which inherently do not express AFP, were infected with an AFP expression vector carried by lentivirus (LV-AFP). 72 h post-infection, approximately 70% of the cells were GFP-positive, indicating high transduction efficiency (Fig. 1B-a). Subsequent puromycin selection and Western blotting analysis revealed significantly increased AFP protein expression in HeLa-AFP cells compared to that in transduced with negative control (NC) vector HeLa-NC and normal HeLa cells ($P < 0.01$) (Fig. 1B-b), the result showed that successfully establishing a HeLa-AFP cell line with stable AFP overexpression. MTT assays were conducted to evaluate the sensitivity of HeLa cells

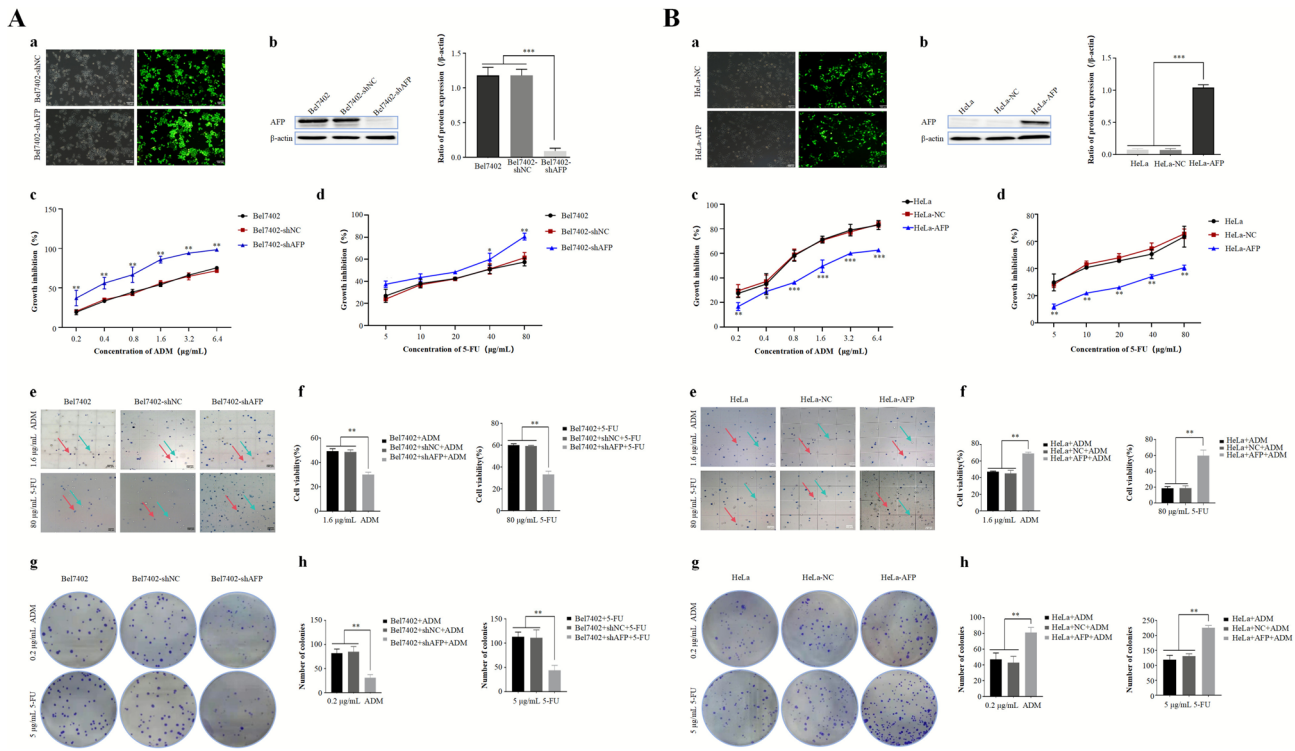


Fig. 1. The effects of the expression of AFP on regulating the chemosensitivity of Bel7402 and HeLa cells. A: (a) Green fluorescent protein expression was used to observe the transduction efficiency of empty lentiviral vector (NC) or lentivirus LV-shAFP on Bel7402 cells. (b) Western blotting was employed to detect the expression of AFP in Bel7402-shAFP cells. After treating Bel7402, Bel7402-shNC, and Bel7402-shAFP cells with different concentrations of ADM (c) and different concentrations of 5-FU (d) for 48 h, the cells growth inhibition rate was calculated. (e) Trypan blue staining was utilized to observe the cellular morphology of Bel7402, Bel7402-shNC, and Bel7402-shAFP cells after treated with 1.6 $\mu\text{g}/\text{mL}$ ADM (upper) and 80 $\mu\text{g}/\text{mL}$ 5-FU (lower) for 48 h (blue arrows indicate living cells, and red arrows indicate dead cells); and (f) the changes in the cells survival rates of each group were calculated. (g) Plate cloning was performed to observe the colony formation of Bel7402, Bel7402-shNC, and Bel7402-shAFP cells after treated with 0.2 $\mu\text{g}/\text{mL}$ ADM (upper) and 5 $\mu\text{g}/\text{mL}$ 5-FU (lower); and (h) the numbers of the cell colonies formed in each group was statistically analyzed. B: (a) Green fluorescent protein expression was used to observe the transduction efficiency of empty lentiviral vector (NC) or lentivirus LV-AFP on HeLa cells. (b) Western blotting was employed to detect the expression of AFP protein in HeLa-AFP cells. After treating HeLa, HeLa-NC, and HeLa-AFP cells with different concentrations of ADM (c) and different concentrations of 5-FU (d) for 48 h, the cells growth inhibition rate was calculated. (e) Trypan blue staining was utilized to observe the cellular morphology of HeLa, HeLa-NC, and HeLa-AFP cells after stimulation with 1.6 $\mu\text{g}/\text{mL}$ ADM (upper) and 80 $\mu\text{g}/\text{mL}$ 5-FU (lower) for 48 h (blue arrows indicate living cells, and red arrows indicate dead cells); and (f) the changes in the cells survival rates of each group were calculated. (g) Plate cloning was performed to observe the colony formation of HeLa, HeLa-NC, and HeLa-AFP cells after treated with 0.2 $\mu\text{g}/\text{mL}$ ADM (upper) and 5 $\mu\text{g}/\text{mL}$ 5-FU (lower); and (h) the numbers of the cell colonies formed in each group was statistically analyzed. The results represented in the figure are derived from three independent experiments ($n=3$). * $P<0.05$, ** $P<0.01$.

to ADM and 5-FU following AFP overexpression. The results showed that the growth inhibition rate of HeLa-AFP cells was significantly lower than that of normal HeLa and HeLa-NC cells when treated with different concentrations of ADM and 5-FU ($P<0.05$, $P<0.01$) (Fig. 1B-c, d), suggesting that AFP overexpression may reduce the sensitivity of HeLa cells to ADM and 5-FU. HeLa-AFP cells exhibited significantly higher survival rates under treatment with 1.6 $\mu\text{g}/\text{mL}$ ADM and 80 $\mu\text{g}/\text{mL}$ 5-FU (Fig. 1B-e, f) and formed more colonies under treatment with 0.2 $\mu\text{g}/\text{mL}$ ADM and 5 $\mu\text{g}/\text{mL}$ 5-FU than normal HeLa and HeLa-NC cells ($P<0.01$), indicating that AFP overexpression may confer resistance to chemotherapeutic drugs by promoting cell proliferation and thus facilitating HeLa cell resistance to ADM and 5-FU (Fig. 1B-g, h). In contrast to the interference of the expression of AFP, AFP overexpression exhibited the opposite effect on chemosensitivity. Overexpression of AFP was able to reduce the sensitivity of HeLa cells to chemotherapeutic drugs.

The effect of AFP expression on apoptosis and chemosensitivity of Bel7402 and HeLa cell

We further explored the effects of AFP silencing and overexpression on the apoptotic response and sensitivity changes in Bel7402 and HeLa cells while treated with chemotherapeutic drugs. Cells from each group were treated individually with 1.6 $\mu\text{g}/\text{mL}$ ADM and 80 $\mu\text{g}/\text{mL}$ 5-FU. After 48 h of drug exposure, TUNEL and DAPI staining

was performed, and cellular morphological changes were observed under an inverted fluorescence microscope. In the Bel7402 cell line, as shown in Fig. 2A-a and Fig. 2A-b, Bel7402-shAFP cells exhibited significant apoptotic features following drug treatment, including decreased nuclear (blue) volume, irregular morphology, nuclear condensation, and nuclear fragmentation. Moreover, the numbers of TUNEL-labeled apoptotic nuclei (red) were significantly higher than in normal Bel7402 and Bel7402-shNC cells. These results indicated that silencing the expression of AFP could enhance the sensitivity of Bel7402 cells to ADM and 5-FU. In contrast, we observed a starkly different phenomenon in HeLa cells. As shown in Fig. 2B-a and Fig. 2B-b, although normal HeLa and HeLa-NC cells also exhibited apoptotic features, such as nuclear condensation following drug treatment, the numbers of TUNEL-labeled apoptotic nuclei were significantly reduced in the HeLa-AFP cells group compared to that in normal HeLa and HeLa-NC cells. The results suggested that AFP overexpression may enhance drug resistance in HeLa cells by inhibiting the apoptotic pathways, thereby reducing their sensitivity to ADM and 5-FU.

Bioinformatics analysis of AFP regulated the PI3K/Akt/NF- κ B signaling pathway in HCC and cervical cancer

To further elucidate the biological significance of AFP and its role in regulating the PI3K/Akt/NF- κ B signaling pathway, we conducted comprehensive investigations of both HCC and cervical cancer by integrating bioinformatics analyses and laboratory experiments.

We began with bioinformatics analyses to explore AFP-related molecular signatures. In HCC, whole-genome expression profiling via the LinkedOmics database identified 10,715 AFP-associated genes (Fig. 3A-a), which

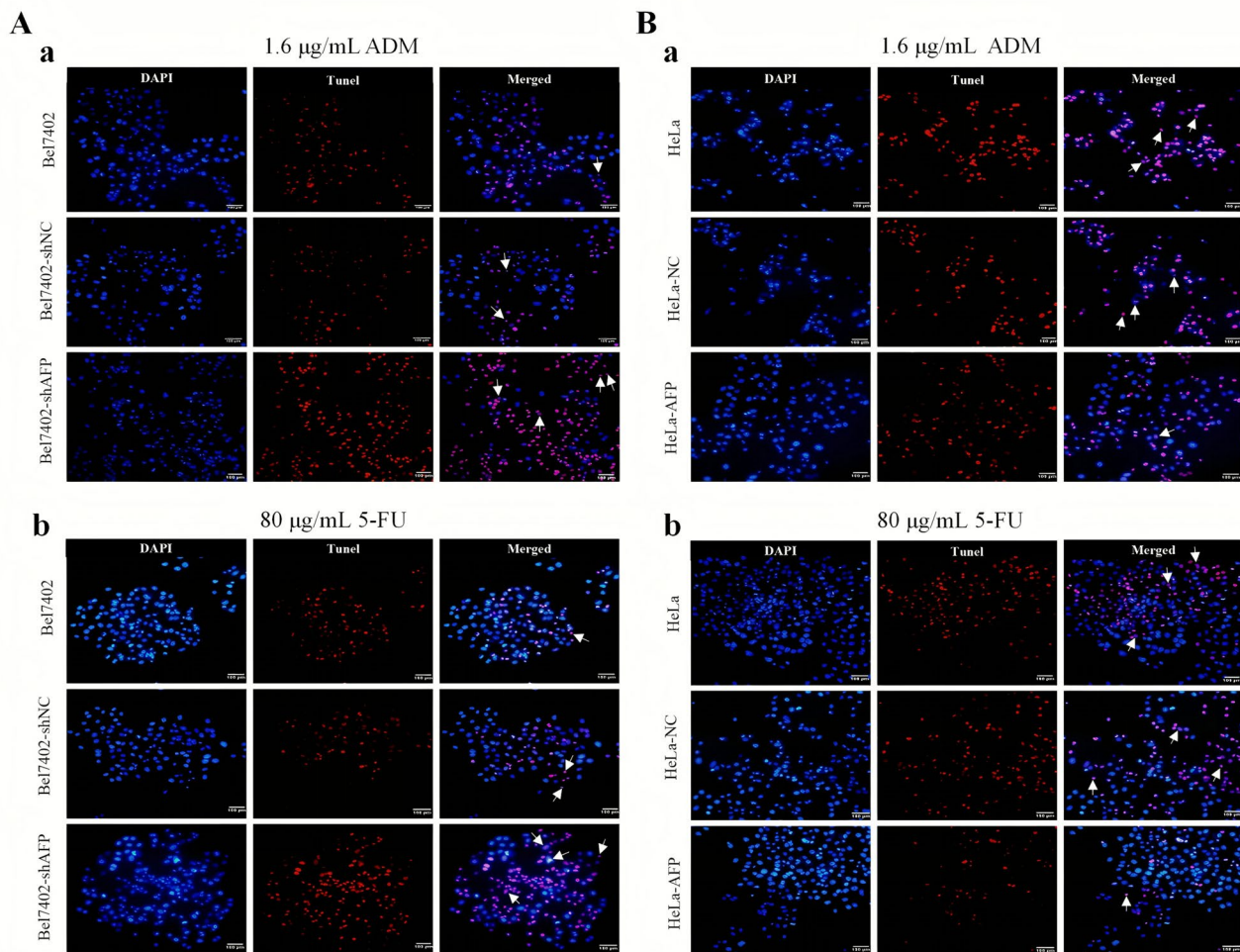


Fig. 2. Effects of AFP on regulating the apoptosis of Bel7402 and HeLa cells under treated with drugs. A: After treated Bel7402, Bel7402-shNC, and Bel7402-shAFP cells with 1.6 μ g/mL ADM (a) or 80 μ g/mL 5-FU (b) for 48 h, TUNEL was used to detect the apoptosis of cells in each group. B: After treated HeLa, HeLa-NC, and HeLa-AFP cells with 1.6 μ g/mL ADM (c) or 80 μ g/mL (d) 5-FU for 48 h, TUNEL was used to detect the apoptosis of cells in each group. The white arrows in the figure indicate representative apoptotic cells. The data represent three independent experiments. The results represented in the figure are derived from three independent experiments ($n = 3$).

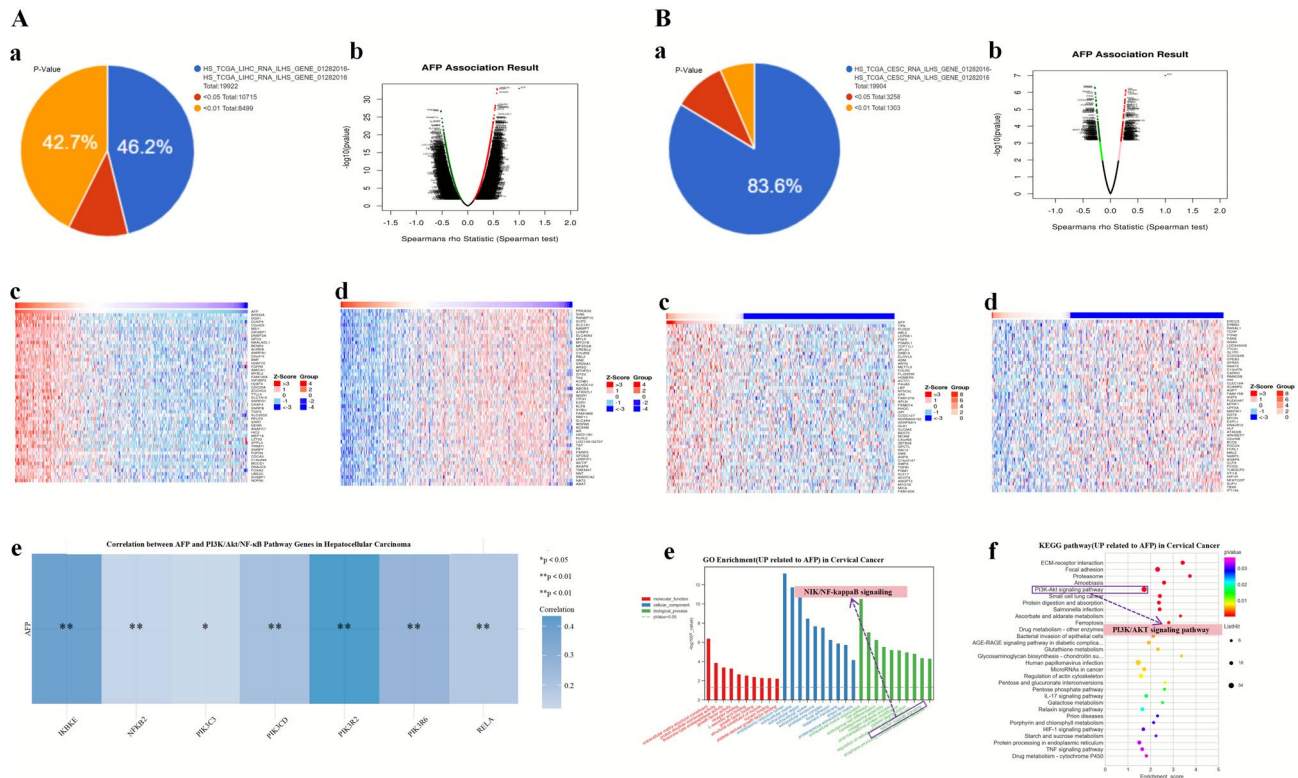


Fig. 3. Bioinformatics analyze the association between AFP and the expression of other genes in HCC and cervical cancer. A: (a) Overview of AFP-related genes in HCC (LinkedOmics database). (b) Volcano plot of AFP-related genes in HCC. (c) Heatmap of AFP positively correlated genes in HCC. (d) Heatmap of AFP negatively correlated genes in HCC. (e) Correlation analysis of AFP and some related-genes of PI3K/Akt/NF-κB in HCC (Clinical Bioinformatics Hub). B: (a) Overview of AFP-related genes in cervical cancer (LinkedOmics database). (b) Volcano plot of AFP-related genes in cervical cancer. (c) Heatmap of some AFP positively correlated genes in cervical cancer. (d) Heatmap of some AFP negatively correlated genes in cervical cancer. (e) GO function analysis of AFP negatively correlated genes in cervical cancer. (f) KEGG pathway enrichment analysis of AFP negatively correlated genes in cervical cancer.

were categorized into positively and negatively correlated clusters (Fig. 3A-b-d). While initial GO and KEGG analyses did not reveal enrichment in the PI3K/Akt/NF-κB pathway, a focused investigation of the TCGA-LIHC dataset through the Clinical Bioinformatics Home platform uncovered significant positive correlations between AFP and key pathway components, including IKBKE, NFKB2, PIK3C3, PIK3CD, PIK3R2, PIK3R6, and RELA (Fig. 3A-e).

Extending these bioinformatics analyses to cervical cancer, we used LinkedOmics to identify 3,258 AFP-associated genes ($P < 0.05$) (Fig. 3B-a), which were stratified into positive and negative correlation groups (Fig. 3B-b,c,d). GO and KEGG enrichment analyses, conducted with the assistance of the DAVID database and Ouyang Cloud tool, showed that AFP-positively correlated genes were predominantly involved in NF-κB signaling, cell adhesion, and growth activation factors, with significant enrichment in the PI3K/Akt signaling pathway (Fig. 3B-e). Bioinformatics analysis using the KEGG pathway database showed that the important signaling pathways closely related to AFP in cervical cancer cells were the PI3K/AKT signaling pathway, suggesting that AFP might promote drug resistance in cancer cells by regulating the PI3K/AKT signaling pathway (Fig. 3B-f).

Building on these bioinformatics insights, we performed experimental validations, starting with HCC. Using the Bel7402 cell line, immunofluorescence staining first revealed reduced nuclear translocation of p65 in AFP-silenced Bel7402-shAFP cells—an indicator of NF-κB pathway inhibition (Fig. 4A). We further validated this with Western blotting: AFP silencing led to a significant decrease in the expression of phosphorylated Akt (p-Akt) and phosphorylated p65 (p-p65) ($P < 0.01$), while the total protein levels of Akt and p65 remained unchanged (Fig. 4B). To confirm the dependence of this pathway on PI3K activity, we treated cells with the PI3K inhibitor LY294002, which significantly downregulated both p-Akt and p-p65 expression ($P < 0.01$) (Fig. 4B). These results collectively confirm AFP's pivotal regulatory role in the PI3K/Akt/NF-κB pathway in HCC.

We then extended experimental validations to cervical cancer to verify a conserved mechanism. In HeLa cells, immunofluorescence staining showed marked enhancement of p65 nuclear translocation in AFP-overexpressing HeLa-APP cells compared to parental HeLa and HeLa-NC cells (Fig. 4C)—consistent with NF-κB pathway activation. Western blotting further supported this: HeLa-APP cells exhibited significantly elevated p-Akt and p-p65 expression ($P < 0.01$) relative to control cells (Fig. 4D). Treatment with LY294002 effectively suppressed

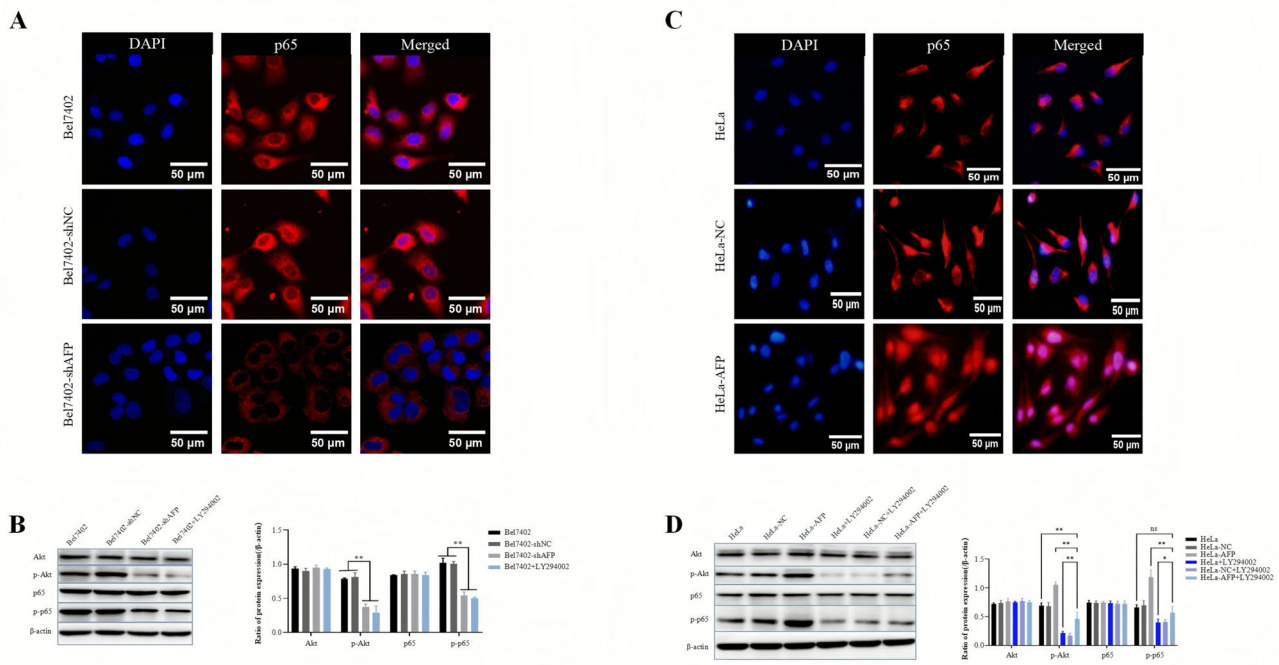


Fig. 4. The effect of AFP on the activation of PI3K/Akt/NF-κB signaling pathway in HCC cells and cervical cancer cells. A: Immunofluorescence was used to observe the localization of p65 in Bel7402, Bel7402-shNC, and Bel7402-shAFP cells. B: Bel7402, Bel7402-shNC, and Bel7402-shAFP cells were treated with PI3K inhibitor LY294002 for 12 h, Western blotting was used to detect the expression changes of PI3K/Akt/NF-κB signaling pathway-related proteins. C: Immunofluorescence was used to observe the localization of p65 in HeLa, HeLa-NC, and HeLa-AFP cells. D: HeLa, HeLa-NC, and HeLa-AFP cells were treated with PI3K inhibitor LY294002 for 12 h, Western blotting was used to detect the expression changes of PI3K/Akt/NF-κB signaling pathway-related proteins. The results represented in the figure are derived from three independent experiments ($n=3$). ** $P<0.01$.

p-Akt and p-p65 expression in all three cell types ($P<0.01$) (Fig. 4D), confirming that AFP activates the PI3K/Akt/NF-κB pathway in cervical cancer as well. Notably, the p-Akt levels in HeLa-AFP + LY294002 group were significantly lower than those in untreated HeLa controls ($P<0.01$), while no statistically significant difference in p-p65 levels was observed between HeLa-AFP + LY294002 and HeLa groups ($P>0.05$) (Fig. 4D). Importantly, comparative analysis revealed persistent AFP-mediated pathway activation under inhibitor treatment: both p-Akt and p-p65 levels in HeLa-AFP + LY294002 group remained significantly higher than those in HeLa + LY294002 group ($P<0.01$), with the p-p65 elevation showing particular prominence ($P<0.05$) (Fig. 4D). These differential responses highlight that while LY294002 effectively suppresses baseline PI3K/Akt signaling, AFP overexpression maintains partial pathway activation even under pharmacological inhibition.

Effect of AFP on RELA (p65)-mediated regulation of MDR and anti-apoptotic gene expression in HCC and cervical cancer cells

To explore the relationships between the RELA (p65) gene, ABC transporters (ABCB1/MDR1, ABCC1/MRP1, and ABCG2/BCRP), anti-apoptotic genes (BIRC2/cIAP1, BIRC7/Livin, and XIAP), and AFP in HCC and cervical cancer, we adopted an integrated approach combining bioinformatics and laboratorial experiments verification. In both HCC and cervical cancer, initial investigations using the GEPIA database revealed correlations between RELA (p65) and ABC transporters and anti-apoptotic genes. In HCC, RELA (p65) was correlated with ABCB1, ABCC1, ABCG2, BIRC2, BIRC7, and XIAP, with high positive correlations for ABCC1, BIRC2, and XIAP ($R>0.3$) (Fig. 5A-a). Using mRNA sequence data from 371 TCGA samples, a multi-gene expression correlation heatmap (generated using the R package pheatmap) confirmed positive correlations between RELA (p65) and ABCB1, ABCC1, BIRC2, BIRC7, and XIAP (Fig. 5A-b). In the HCC cell line Bel7402, compared with normal Bel7402 and Bel7402-shNC cells, the expression levels of ABC transporters MDR1, MRP1, BCRP, and anti-apoptotic genes XIAP, cIAP1, and Livin were significantly reduced in Bel7402-shAFP cells ($P<0.01$) (Fig. 5A-c). Regarding the role of the PI3K/Akt/NF-κB pathway, treatment of Bel7402 cells with the PI3K inhibitor LY294002 at 50 μ mol/L for 12 h led to a significant decrease in the protein expression of MDR1, MRP1, BCRP, XIAP, cIAP1, and Livin ($P<0.01$), similar to the effects of AFP silencing (Fig. 5A-c).

In cervical cancer, RELA (p65) was correlated with ABCB1, ABCC1, ABCG2, BIRC2, and XIAP, with high positive correlations for ABCC1, BIRC2, and XIAP ($R>0.03$) (Fig. 5B-a). Analysis of mRNA sequence data from 306 TCGA samples also confirmed consistency with the GEPIA results (Fig. 5B-b). In the cervical cancer cell line HeLa, in HeLa-AFP cells, the expression levels of MDR1, MRP1, BCRP, XIAP, cIAP1, and Livin were significantly

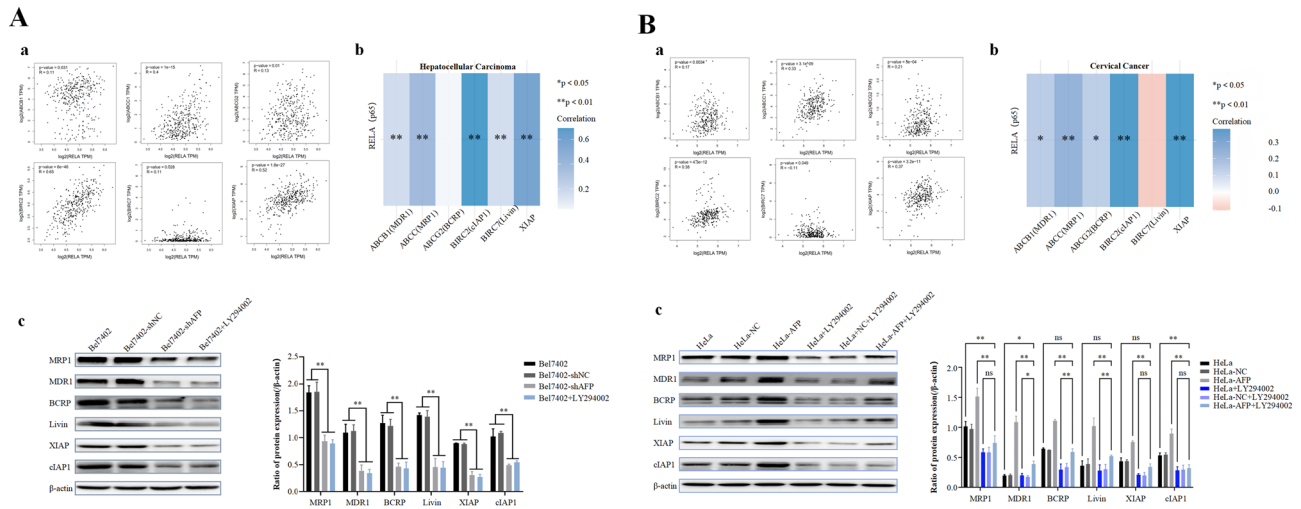


Fig. 5. The influence of AFP on regulating RELA(p65)-mediated MDR and anti-apoptotic gene expression in HCC and cervical cancer cells. **A:** (a) Spearman correlation analysis of two genes, RELA and ABCB1, RELA and ABCC1, RELA and ABCG2, RELA and BIRC2, RELA and BIRC7, and RELA and XIAP in HCC. (b) Spearman correlation analysis of multiple genes, RELA and ABCB1, ABCC1, ABCG2, BIRC2, BIRC7, and XIAP in HCC. (c) Bel7402, Bel7402-shNC, and Bel7402-shAFP cells were treated with PI3K inhibitor LY294002 for 12 h, Western blotting was used to detect the changes in the expression of various drug resistance genes. **B:** (a) Spearman correlation analysis of two genes, RELA and ABCB1, RELA and ABCC1, RELA and ABCG2, RELA and BIRC2, RELA and BIRC7, and RELA and XIAP in cervical cancer. (b) Spearman correlation analysis of multiple genes, RELA and ABCB1, ABCC1, ABCG2, BIRC2, BIRC7, and XIAP in cervical cancer. (c) HeLa, HeLa-NC, and HeLa-AFP cells were treated with PI3K inhibitor LY294002 for 12 h, Western blotting was used to detect the changes in the expression of various drug resistance genes. The results represented in the figure are derived from three independent experiments ($n = 3$). ** $P < 0.01$.

elevated ($P < 0.01$) (Fig. 5B-c). In normal HeLa, HeLa-NC, and HeLa-AFP cells, treatment with LY294002 for 12 h also significantly reduced the expression of MDR1, MRP1, BCRP, XIAP, cIAP1, and Livin ($P < 0.01$) (Fig. 5B-c). Strikingly, inhibitor-treated HeLa-AFP cells exhibited target-specific modulation: MRP1 and cIAP1 levels in the HeLa-AFP + LY294002 group were significantly lower than in untreated HeLa controls ($P < 0.05$ and $P < 0.01$, respectively) (Fig. 5B-c), demonstrating a "hyper-suppressive" effect. In contrast, MDR1 expression in the HeLa-AFP + LY294002 group remained elevated compared to HeLa controls ($P < 0.05$) (Fig. 5B-c), indicating incomplete pathway reversal. Notably, BCRP, Livin, and XIAP levels showed no significant differences between HeLa-AFP + LY294002 and untreated HeLa groups ($P > 0.05$) (Fig. 5B-c), suggesting full restoration to baseline. Comparative analysis under PI3K inhibition further revealed persistent AFP-mediated resistance signals: BCRP, MDR1, and Livin expression in the HeLa-AFP + LY294002 group remained significantly higher than in the HeLa + LY294002 control group ($P < 0.01$) (Fig. 5B-c), highlighting AFP's ability to sustain partial drug resistance even during pathway suppression.

Discussion

Cancer is a fatal disease that accounts for countless lives annually. The complexity and heterogeneity of cancer necessitate diverse treatment strategies, with chemotherapy being one of the primary therapeutic approaches¹⁸. However, the efficacy of chemotherapy has been severely challenged by MDR. MDR refers to the cross-resistance of cancer cells to one or more chemotherapeutic drugs with different mechanisms of action⁶. The emergence of MDR not only limits the therapeutic effectiveness of chemotherapeutic drugs, but also increases the difficulty and value of treatment, posing a significant threat to the quality of life and survival rates of patients¹⁹.

AFP is a liver synthesized protein with specificity during the embryonic period, and its baseline level in adults is typically very low²⁰. However, the serum concentration of AFP significantly increases during cancer progression, particularly HCC, making it a key biomarker for assessing tumor activity and recurrence²¹. As a tumor marker, AFP has a variety of biological functions. It is involved in numerous physiological processes such as protein synthesis and amino acid transport, which are essential for maintaining normal cellular metabolism²². Moreover, AFP has been found to promote the proliferation of tumor cells, enhance their invasiveness and migratory capacity, and influence the development and metastasis of cancer cells by modulating the tumor microenvironment^{10,11}. While the role of AFP in tumor progression and HCC has been extensively studied, its role in multidrug resistance (MDR) remains less explored. Several studies have suggested that AFP may be involved in the regulation of drug resistance pathways, such as the Wnt/β-catenin and PI3K/AKT pathways, in hepatocellular carcinoma (HCC)^{23,24}. However, the specific mechanisms underlying the relationship between AFP and MDR remain largely unclear. In this study, we investigated the role of AFP in MDR in a broader range of cancer types, including cervical cancer, and found that interference with the expression of AFP could enhance

the sensitivity of Bel7402 to ADM and 5-FU, while overexpression of AFP could inhibit the sensitivity of cervical cancer cells to ADM and 5-FU, suggesting that AFP may be involved in the MDR of cancer cells.

To rigorously assess AFP's role in chemoresistance, we optimized drug concentrations based on preliminary dose-response curves. For acute cytotoxicity and apoptosis assays (MTT, TUNEL; 48–72 h), higher concentrations (1.6 μ g/mL ADM, 80 μ g/mL 5-FU) were selected to induce 50–80% inhibition in parental cells. These doses provided sufficient dynamic range to detect AFP-mediated resistance differences while avoiding complete cell death. In contrast, long-term colony formation assays employed sub-lethal concentrations (0.2 μ g/mL ADM, 5 μ g/mL 5-FU), which mimic the persistent low-dose chemotherapy exposure observed clinically. This approach selectively allowed survival and proliferation of resistant subpopulations, effectively revealing AFP's role in sustaining drug-tolerant clones.

Increased drug efflux is a crucial mechanism of MDR²⁵. Tumor cells express a variety of drug transport proteins such as P-glycoprotein (P-gp) and MDR-associated proteins (MRPs), which extrude chemotherapeutic agents from cancer cells, thereby reducing the cytotoxic effects of drugs^{25,26}. The expression of these transporters is often influenced by gene regulatory networks in tumor cells, including transcription factors, signaling pathways, and epigenetic modifications. Apoptosis inhibition is an important mechanism for MDR development⁷. Chemotherapeutic drugs typically aim to induce apoptosis in cancer cells for therapeutic purposes. Cancer cells can suppress the apoptotic process through multiple pathways, such as by upregulating the expression of anti-apoptotic proteins, downregulating the expression of pro-apoptotic proteins, or activating anti-apoptotic signaling pathways. These changes can confer resistance to chemotherapeutic drugs, thereby reducing the drug efficacy.

Our preliminary studies showed that AFP is associated with various biological behaviors of cancer cells and can regulate the expression of multiple related proteins^{24,27–29}. However, whether AFP regulates the expression of MDR- and apoptosis-related proteins remains unclear. In this study, we further investigated the effect of AFP on the expression of MDR- and apoptosis-related proteins using Western blotting. The results indicated that overexpression of AFP was able to promote the expression of MDR proteins, MDR1, MRP1, and BCRP, and apoptosis-inhibiting proteins XIAP, cIAP1, and Livin in HCC cells. Further analysis of these proteins revealed nuanced regulatory mechanisms. For MRP1 and cIAP1, AFP overexpression combined with PI3K inhibition (LY294002) caused levels to drop below baseline in HeLa cells ($P < 0.05$, $P < 0.01$), indicating complete pathway dependency. In contrast, MDR1 remained elevated in HeLa-AFP + LY294002 vs. controls ($P < 0.05$), suggesting partial reliance on non-PI3K pathways. BCRP, Livin, and XIAP reverted to baseline ($P > 0.05$), reflecting classical linear PI3K dependency. Strikingly, when comparing HeLa-AFP + LY294002 to HeLa + LY294002, BCRP, MDR1, and Livin remained elevated, highlighting AFP's redundant regulatory networks. These findings demonstrate that AFP orchestrates resistance through a PI3K/Akt/NF- κ B “core” while employing backup mechanisms for select targets, underscoring the complexity of its MDR network.

While prior studies have established that AFP activates PI3K/Akt signaling and promotes NF- κ B nuclear translocation in HCC models^{23,24}, our study extends this knowledge by systematically modulating AFP expression in both hepatic (Bel7402) and non-hepatic (HeLa) cancer cells. We demonstrate that AFP overexpression universally enhances MDR across these distinct lineages, whereas AFP knockdown sensitizes Bel7402 cells to chemotherapy. This functional conservation underscores AFP's broader role as an oncogenic amplifier beyond its tissue-specific origins.

Our previous studies have demonstrated that AFP could activate the PI3K/AKT signaling pathway, and the PI3K/AKT signaling pathway is involved in the regulation of MDR-related genes and apoptosis-related genes^{30,31}. Many studies have shown that activation of the PI3K/AKT signaling pathway is positively correlated with MDR in HCC, such as HCC resistance to atezolizumab and bevacizumab³², lenvatinib^{33,34}, sorafenib³⁵, doxorubicin³⁶, regorafenib³⁷, and 5-FU³⁸. The PI3K/AKT signaling pathway that activates NF- κ B also leads to HCC resistance to drug therapy^{39–42}. These findings suggest that the activation of PI3K/AKT/NF- κ B signaling pathway plays a key role in drug resistance in liver cancer⁴³. Although our previous studies have found that AFP activates the PI3K/AKT signaling pathway by inhibiting the activity of PTEN²⁷, whether AFP promotes drug resistance in HCC cells through the PI3K/AKT signaling pathway is still unclear. Western blot analysis of pAKT and p65 provided critical mechanistic insights. In HeLa-AFP cells treated with LY294002 (PI3K inhibitor), p-AKT levels dropped below those of parental HeLa cells, revealing “oncogene addiction”—AFP-overexpressing cells rely excessively on PI3K/Akt signaling for survival. Conversely, p-p65 levels in HeLa-AFP + LY294002 showed no significant difference vs. HeLa controls, confirming that AFP-driven NF- κ B activation is PI3K-dependent. Notably, HeLa-AFP + LY294002 maintained higher p-AKT and p-p65 levels than HeLa + LY294002, suggesting AFP retains weak PI3K-independent activation mechanisms. This dual dependency underscores AFP's ability to sustain survival signals even under pathway inhibition. The observed discrepancies may also stem from AFP-mediated PTEN inhibition in HeLa-AFP + LY294002 cells, which creates a PI3K activation bias compared to HeLa + LY294002 cells with intact PTEN, thereby diminishing LY294002 efficacy.

To explore whether AFP regulates MDR in cancer cells by activating the PI3K/AKT signaling pathway, and to elucidate the detailed mechanism by which AFP regulates the expression of ABC transporters and anti-apoptotic genes, we conducted a bioinformatics analysis. In cervical cancer, GO functional analysis showed that the genes co-expressed with AFP were involved in biological processes, such as NF- κ B signaling, and KEGG enrichment analysis indicated that the genes co-expressed with AFP were enriched in the PI3K/Akt signaling pathway. In HCC, AFP is positively correlated with some related-genes of the PI3K/Akt/NF- κ B signaling pathway (a downstream component of PI3K/Akt/NF- κ B axis)^{27,44}. Further analysis revealed that the core factors of NF- κ B and p65 were correlated with the resistance genes MDR1, MRP1, BCRP, XIAP, cIAP1, and Livin. Therefore, we hypothesized that AFP regulates the expression of ABC transporters and anti-apoptotic genes by modulating NF- κ B signaling through activating the PI3K/Akt signaling pathway. Western blotting, immunofluorescence

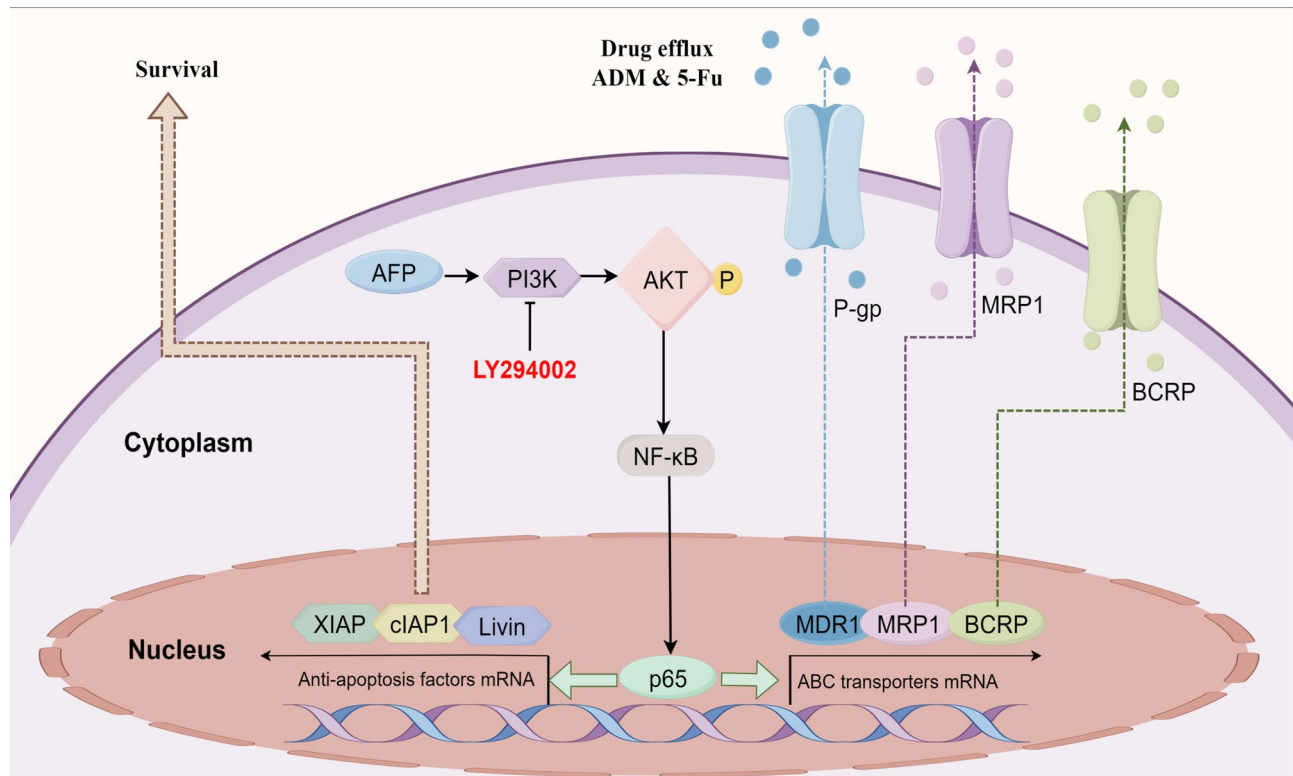


Fig. 6. Involved molecular mechanism of AFP promoting MDR in cancer cells. AFP can activate the PI3K/Akt/NF-κB signaling pathway, and the activation of this pathway further promotes the activation of NF-κB. The activated NF-κB, such as p65, can translocate into the nucleus. After p65 translocates into the nucleus, on the one hand, it can stimulate the transcription of drug resistance genes, thereby increasing the efflux of chemotherapeutic drugs; on the other hand, it can promote the expression of anti-apoptotic genes, thus enhancing the survival ability of cancer cells.

assays, and the use of pathway inhibitors further confirmed that AFP could activate the PI3K/Akt/NF-κB signaling pathway, promoting the nuclear translocation of the key factor p65 in the NF-κB pathway.

Confirming AFP's established role in NF-κB activation^{27,44}, we observed that AFP overexpression/interference in HeLa/Bel7402 cells significantly increased/ decreased p65 phosphorylation and nuclear translocation (Fig. 4). Importantly, this effect correlated with upregulated/downregulated MDR1 and XIAP expression in a cell type-independent manner, directly linking AFP-driven NF-κB activity to functional chemoresistance phenotypes across lineages.

While AFP's pro-tumorigenic effects are well-documented in HCC, our deliberate manipulation of AFP levels in cervical cancer (HeLa) cells revealed its capacity to induce a comparable MDR phenotype. This cross-lineage validation—achieved through both gain-of-function (HeLa-AFP) and loss-of-function (Bel7402 shAFP) approaches—positions AFP as a pan-cancer resilience factor rather than a liver-specific adaptation.

In summary, our study preliminarily revealed a potential role of AFP in the development of MDR, the schematic diagram of the mechanism by which AFP promotes MDR in cancer cells as showed in Fig. 6. Our findings suggest that AFP may be involved in the progression of MDR by modulating the activity of ABC transporters and expression of anti-apoptotic genes, promoting the efflux of chemotherapeutic drugs, and inhibiting apoptosis. Moreover, AFP may be associated with the activation of the PI3K/Akt/NF-κB signaling pathway, which plays a central role in cell survival and the development of drug resistance. By recapitulating AFP-mediated MDR in controlled cellular systems, we provide experimental validation of its mechanistic conservation across cancer types. These models enable future dissection of AFP's context-dependent interactions, offering a platform for testing AFP-targeted adjuvant therapies to reverse chemoresistance. However, it is essential to recognize that the generation of MDR tumors is an extremely complex process that potentially involves multiple molecular mechanisms and interactions between signaling pathways. In this study, we found that AFP not only plays a pivotal role in stimulating MDR in HCC, but also promotes MDR in cervical cancer. These results demonstrate that AFP is a key molecule that promotes drug resistance in cancer cells, implying that targeted inhibition of AFP expression combined with other drug treatments is a very promising therapeutic strategy in the cancer which expression of AFP.

Data availability

The original data generated in this study are included in the article. If necessary, the corresponding author can be directly contacted.

Received: 12 June 2025; Accepted: 21 November 2025

Published online: 29 November 2025

References

- Shen, C., Jiang, X., Li, M. & Luo, Y. Hepatitis virus and hepatocellular carcinoma: Recent advances. *Cancers (Basel)*. **15**(2), 533. <https://doi.org/10.3390/cancers15020533> (2023).
- Östensson, E. et al. Barriers to and facilitators of compliance with clinic-based cervical cancer screening: population-based cohort study of women aged 23–60 years. *PLoS ONE* <https://doi.org/10.1371/journal.pone.0128270> (2015).
- Khare, S., Khare, T., Ramanathan, R. & Ibdah, J. A. Hepatocellular carcinoma: The role of microRNAs. *Biomolecules* **12**(5), 645. <https://doi.org/10.3390/biom12050645> (2022).
- Li, Y., Zhang, R., Xu, Z. & Wang, Z. Advances in nanoliposomes for the diagnosis and treatment of liver cancer. *Int. J. Nanomed.* **17**, 909–925. <https://doi.org/10.2147/IJN.S349426> (2022).
- Wu, S. et al. Molecular mechanisms of long noncoding RNAs associated with cervical cancer radiosensitivity. *Front Genet.* **13**, 1093549. <https://doi.org/10.3389/fgene.2022.1093549> (2023).
- Russo, A., Saide, A., Smaldone, S., Faraonio, R. & Russo, G. Role of uL3 in multidrug resistance in p53-mutated lung cancer cells. *Int. J. Mol. Sci.* **18**(3), 547. <https://doi.org/10.3390/ijms18030547> (2017).
- Jovanović, M., Podolski-Renić, A., Krasavina, M. & Pešić, M. The role of the thioredoxin detoxification system in cancer progression and resistance. *Front Mol. Biosci.* <https://doi.org/10.3389/fmolt.2022.883297> (2022).
- Lei, Z. N. et al. Establishment and characterization of a Topotecan resistant non-small cell lung cancer NCI-H460/TPT10 cell line. *Front Cell Dev. Biol.* <https://doi.org/10.3389/fcell.2020.607275> (2020).
- Feder, S., Kandulski, A., Schacherer, D., Weiss, T. S. & Buechler, C. Serum chemerin does not differentiate colorectal liver metastases from hepatocellular carcinoma. *Int. J. Mol. Sci.* **20**(16), 3919. <https://doi.org/10.3390/ijms20163919> (2019).
- Teng, W. et al. Combination of CRAFITY score with alpha-fetoprotein response predicts a favorable outcome of atezolizumab plus bevacizumab for unresectable hepatocellular carcinoma. *Am. J. Cancer Res.* **12**(4), 1899–1911 (2022).
- Shimamura, T., Goto, R., Watanabe, M., Kawamura, N. & Takada, Y. Liver transplantation for hepatocellular carcinoma: How should we improve the thresholds?. *Cancers (Basel)*. **14**(2), 419. <https://doi.org/10.3390/cancers14020419> (2022).
- Liu, J. et al. HBx Drives Liver Cancer Stem Cell Generation Through Stimulating Glucose Metabolic Reprogramming. *J. Cell. Mol. Med.* <https://doi.org/10.1111/jcmm.70722> (2025).
- Lu, Y. et al. Alpha fetoprotein plays a critical role in promoting metastasis of hepatocellular carcinoma cells. *J. Cell Mol. Med.* **20**(3), 549–558. <https://doi.org/10.1111/jcmm.12745> (2016).
- Wang, W. et al. Ropivacaine promotes apoptosis of hepatocellular carcinoma cells through damaging mitochondria and activating caspase-3 activity. *Biol. Res.* **52**(1), 36. <https://doi.org/10.1186/s40659-019-0242-7> (2019).
- Wang, S. et al. Targeting ACYP1-mediated glycolysis reverses lenvatinib resistance and restricts hepatocellular carcinoma progression. *Drug Resist. Updat.* <https://doi.org/10.1016/j.drup.2023.100976> (2023).
- Zeng, Y., Cui, Z., Liu, J., Chen, J. & Tang, S. MicroRNA-29b-3p Promotes Human Retinal Microvascular Endothelial Cell Apoptosis via Blocking SIRT1 in Diabetic Retinopathy. *Front Physiol.* **29**(10), 1621. <https://doi.org/10.3389/fphys.2019.01621> (2020).
- Shan, Q. et al. The p-MYH9/USP22/HIF-1 α axis promotes lenvatinib resistance and cancer stemness in hepatocellular carcinoma. *Signal. Transd. Target Ther.* **9**(1), 249. <https://doi.org/10.1038/s41392-024-01963-5> (2024).
- Yin, X. et al. Serum metabolic fingerprints on bowl-shaped submicroneedle chip for chemotherapy monitoring. *ACS Nano* **16**(2), 2852–2865. <https://doi.org/10.1021/acsnano.1c09864> (2022).
- Winter, S. J., Miller, H. A. & Steinbach-Rankins, J. M. Multicellular ovarian cancer model for evaluation of nanovector delivery in ascites and metastatic environments. *Pharmaceutics*. **13**(11), 1891. <https://doi.org/10.3390/pharmaceutics13111891> (2021).
- Pan, Y. et al. AFP shields hepatocellular carcinoma from macrophage phagocytosis by regulating HuR-mediated CD47 translocation in cellular membrane. *Transl. Oncol.* <https://doi.org/10.1016/j.tranon.2024.102240> (2024).
- Montal, R. et al. Molecular portrait of high alpha-fetoprotein in hepatocellular carcinoma: implications for biomarker-driven clinical trials. *Br. J. Cancer* **121**(4), 340–343. <https://doi.org/10.1038/s41416-019-0513-7> (2019).
- Sarandakou, A., Protonotariou, E. & Rizos, D. Tumor markers in biological fluids associated with pregnancy. *Crit. Rev. Clin. Lab. Sci.* **44**(2), 151–178. <https://doi.org/10.1080/10408360601003143> (2007).
- Shan, X., Zhang, M., Lin, H., Zhu, M. & Li, M. Alpha-fetoprotein Promotes the Malignant Phenotype of Hepatocellular Carcinoma Cells: the Drugs Resistance Origination. *Trends Oncol.* **3**(2), 1–18. <https://doi.org/10.37155/2717-5278-2021-03-02-1> (2021).
- Li, M. et al. Alpha-fetoprotein: a new member of intracellular signal molecules in regulation of the PI3K/AKT signaling in human hepatoma cell lines. *Int. J. Cancer* **128**(3), 524–532. <https://doi.org/10.1002/ijc.25373> (2011).
- Domínguez-Álvarez, E. et al. Identification of selenocompounds with promising properties to reverse cancer multidrug resistance. *Bioorg. Med. Chem. Lett.* **26**(12), 2821–2824. <https://doi.org/10.1016/j.bmcl.2016.04.064> (2016).
- Nasr, R. et al. Molecular analysis of the massive GSH transport mechanism mediated by the human multidrug resistant protein 1/ABCC1. *Sci. Rep.* **10**(1), 7616. <https://doi.org/10.1038/s41598-020-64400-x> (2020).
- Wang, S. et al. Alpha-fetoprotein inhibits autophagy to promote malignant behaviour in hepatocellular carcinoma cells by activating PI3K/AKT/mTOR signalling. *Cell Death Dis.* **9**(10), 1027. <https://doi.org/10.1038/s41419-018-1036-5> (2018).
- Li, M. et al. Alpha-fetoprotein receptor as an early indicator of HBx-driven hepatocarcinogenesis and its applications in tracing cancer cell metastasis. *Cancer Lett.* **330**(2), 170–180. <https://doi.org/10.1016/j.canlet.2012.11.042> (2013).
- Lin, B. et al. Structural basis for alpha-fetoprotein-mediated inhibition of caspase-3 activity in hepatocellular carcinoma cells. *Int. J. Cancer* **141**(7), 1413–1421. <https://doi.org/10.1002/ijc.30850> (2017).
- Manna, D. & Sarkar, D. Multifunctional role of astrocyte elevated gene-1 (AEG-1) in cancer: Focus on drug resistance. *Cancers (Basel)*. **13**(8), 1792. <https://doi.org/10.3390/cancers13081792> (2021).
- Liu, R. et al. PI3K/AKT pathway as a key link modulates the multidrug resistance of cancers. *Cell Death Dis.* **11**(9), 797. <https://doi.org/10.1038/s41419-020-02998-6> (2020).
- Zhu, A. X. et al. Molecular correlates of clinical response and resistance to atezolizumab in combination with bevacizumab in advanced hepatocellular carcinoma. *Nat. Med.* **28**(8), 1599–1611. <https://doi.org/10.1038/s41591-022-01868-2> (2022).
- Wang, S. et al. FBXO32 ubiquitination of SUFU promotes progression and lenvatinib resistance in hepatocellular carcinoma via hedgehog signaling. *Med. Oncol.* **42**(4), 98. <https://doi.org/10.1007/s12032-025-02644-1> (2025).
- Liu, X. et al. EVA1A reverses lenvatinib resistance in hepatocellular carcinoma through regulating PI3K/AKT/p53 signaling axis. *Apoptosis* **29**(7–8), 1161–1184. <https://doi.org/10.1007/s10495-024-01967-0> (2024).
- Sun, Y. et al. S-palmitoylation of PCSK9 induces sorafenib resistance in liver cancer by activating the PI3K/AKT pathway. *Cell Rep.* **40**(7), 111194. <https://doi.org/10.1016/j.celrep.2022.111194> (2022).
- Zhai, X. et al. LRP1B suppresses HCC progression through the NCSTN/PI3K/AKT signaling axis and affects doxorubicin resistance. *Genes Dis.* **10**(5), 2082–2096. <https://doi.org/10.1016/j.gendis.2022.10.021> (2022).
- Yang, H. et al. A feedback loop of PPP and PI3K/AKT signal pathway drives regorafenib-resistance in HCC. *Cancer Metab.* **11**(1), 27. <https://doi.org/10.1186/s40170-023-00311-5> (2023).
- Li, J., Cheng, X., Huang, D. & Cui, R. Six2 regulates the malignant progression and 5-FU resistance of hepatocellular carcinoma through the PI3K/AKT/mTOR pathway and DNMT1/E-cadherin methylation mechanism. *Neoplasma* **71**(5), 451–462. https://doi.org/10.4149/neo_2024_240511N214 (2024).

39. Bomfim, L. M. et al. Ru(II)-based complexes containing 2-thiouracil derivatives suppress liver cancer stem cells by targeting NF-kappaB and Akt/mTOR signaling. *Cell Death Discov.* **10**(1), 270. <https://doi.org/10.1038/s41420-024-02036-w> (2024).
40. Zhou, S., Ma, Y., Xu, R. & Tang, X. Nanoparticles loaded with GSK1059615 combined with sorafenib inhibited programmed cell death 1 ligand 1 expression by negatively regulating the PI3K/Akt/NF-kappaB pathway, thereby reversing the drug resistance of hepatocellular carcinoma to sorafenib. *J. Biomed. Nanotechnol.* **18**(3), 693–704. <https://doi.org/10.1166/jbn.2022.3279> (2022).
41. Gupta, R. et al. Multifaceted role of NF-kappaB in hepatocellular carcinoma therapy: Molecular landscape, therapeutic compounds and nanomaterial approaches. *Environ. Res.* **228**, 115767. <https://doi.org/10.1016/j.envres.2023.115767> (2023).
42. Yan, B. et al. CD146 regulates the stemness and chemoresistance of hepatocellular carcinoma via JAG2-NOTCH signaling. *Cell Death Dis.* **16**(1), 150. <https://doi.org/10.1038/s41419-025-07470-x> (2025).
43. Paskeh, M. D. A. et al. Biological impact and therapeutic perspective of targeting PI3K/Akt signaling in hepatocellular carcinoma: Promises and Challenges. *Pharmacol. Res.* <https://doi.org/10.1016/j.phrs.2022.106553> (2023).
44. Li, Q. T. et al. Alpha-Fetoprotein Regulates the Expression of Immune-Related Proteins through the NF-κB (p65) Pathway in Hepatocellular Carcinoma Cells. *J. Oncol.* **2020**, 9327512. <https://doi.org/10.1155/2020/9327512> (2020).

Acknowledgements

We thank Dr. Junnv Xu for assisting with the bioinformatics analysis.

Author contributions

SF, CZ, and YC jointly participated in the experimental design and execution, contributed to key experimental data and analysis, and drafted the initial manuscript. WL, XD, YZ, XL, FW, and BL were involved in part of the experimental operations and data analysis and assisted in writing and revising the paper. ML and MZ, as project leaders, co-guided the entire research and participated in the experimental design, discussion of the results, and wrote final revision of the manuscript. All the authors have read and approved the final revision of the manuscript.

Funding

This work was supported by the National Natural Science Foundation of China (Nos. 82560459, 82460602, 82573045, and 82060514); the Natural Science Foundation of Hainan Province (No. 824RC517); the Hainan Provincial Graduate Innovation Research project (No. Qhys2023-450); the Hainan Province Science and Technology Special Foundation (No. ZDYF2021SHFZ222).

Declarations

Competing interests

The authors declare no competing interests.

Additional information

Supplementary Information The online version contains supplementary material available at <https://doi.org/10.1038/s41598-025-30207-x>.

Correspondence and requests for materials should be addressed to M.L. or M.Z.

Reprints and permissions information is available at www.nature.com/reprints.

Publisher's note Springer Nature remains neutral with regard to jurisdictional claims in published maps and institutional affiliations.

Open Access This article is licensed under a Creative Commons Attribution-NonCommercial-NoDerivatives 4.0 International License, which permits any non-commercial use, sharing, distribution and reproduction in any medium or format, as long as you give appropriate credit to the original author(s) and the source, provide a link to the Creative Commons licence, and indicate if you modified the licensed material. You do not have permission under this licence to share adapted material derived from this article or parts of it. The images or other third party material in this article are included in the article's Creative Commons licence, unless indicated otherwise in a credit line to the material. If material is not included in the article's Creative Commons licence and your intended use is not permitted by statutory regulation or exceeds the permitted use, you will need to obtain permission directly from the copyright holder. To view a copy of this licence, visit <http://creativecommons.org/licenses/by-nc-nd/4.0/>.

© The Author(s) 2025